Sb surfactant-mediated SiGe graded layers for Ge photodiodes integrated on Si

J. L. Liu[a] and Z. Yang
Quantum Structures Laboratory, Department of Electrical Engineering, University of California at Riverside, Riverside, California 92521

K. L. Wang
Device Research Laboratory, Department of Electrical Engineering, University of California at Los Angeles, Los Angeles, California 90095

(Received 3 May 2005; accepted 6 December 2005; published online 20 January 2006)

High-quality SiGe and Ge thin films were grown on Si substrates by molecular-beam epitaxy using a technique that combines SiGe composition grading and Sb surfactant mediation. Both transmission electron microscopy and Schimmel defect etch measurements show that the Sb surfactant-mediated SiGe graded buffer layers have lower dislocation densities than those without an Sb surfactant. A systematic study of Sb surfactant-mediated graded buffers was carried out. The relationship between the threading dislocation densities and the grading rates of the Sb surfactant-mediated SiGe buffer layers was investigated. Moreover, *p-i-n* Ge photodiodes were fabricated on Si substrates using Sb surfactant-mediated SiGe graded buffer layers. These photodiodes exhibit very low dark current densities of about 0.15 mA/cm^2 at the reverse bias of 1 V and high quantum efficiencies of 50%–72%. © *2006 American Institute of Physics*.
[DOI: 10.1063/1.2163013]

I. INTRODUCTION

Optical fiber communication is one of the fastest growing technologies over the last few years. Its further development demands low-cost optical components that operate in the near-infrared windows of fiber-optic transmission (1.3 and 1.55 μm). The commercial technology is currently based on InGaAs/InP materials. Ge photodetector integrated on Si is an alternative for this purpose owing to its band gap of 0.67 eV and full compatibility with modern Si technology. Nevertheless, the large-scale practical application of this kind of devices is not yet realized due to the difficulty in growth of high-quality Ge films on Si with low threading dislocation densities and smooth surfaces. Figure 1 shows the typical result of direct growth of thick Ge film on Si. The sample was grown at 450 °C and consisted of 100 nm Ge on Si (100) substrate. A very rough surface is observed in the bright-field image [Fig. 1(a)]. The dark-field image [Fig. 1(b)] shows high-density dislocations, which are generated in the Si/Ge interface and penetrated into the top Ge film. Such a kind of film generally induces large leakage currents and thus is not applicable in optoelectronics.

The difficulty of obtaining a high-quality Ge film on Si arises from the 4.2% mismatch between the lattice constants of Si and Ge. When Ge is deposited on Si, it first takes the layer-by-layer format. Each Ge atom finds a Si lattice vertex and sits there. This means that the lattice constant of Ge in the lateral direction is forced to be equal to the lattice constant of Si. Because the Ge lattice constant is larger than that of Si, the compressive strain is built in the Ge film. When the film thickness reaches about 6 Å, the strain energy is so large that the film becomes rough, in other words, the two-dimensional film transforms into three-dimensional islands to accommodate strain. This growth mode is the so-called Stranski-Krastanov mode. High-density islands on the surface are referred to as self-assembled Ge quantum dots. When the film thickness is larger than 20 Å, the film deformation is not enough to accommodate the increased strain energy and misfit dislocations are generated in the interface. These misfit dislocations penetrate through the film and form threading dislocations. The more these dislocations are, the worse the film quality is.

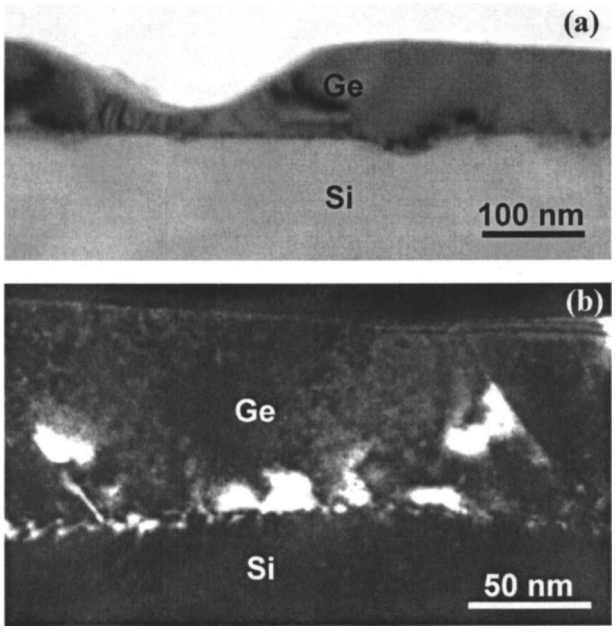

FIG. 1. Direct growth of 100 nm Ge on Si. (a) Bright-field TEM image shows a very rough surface and (b) Dark-field image shows high-density threading dislocations.

[a]Electronic mail: jianlin@ee.ucr.edu

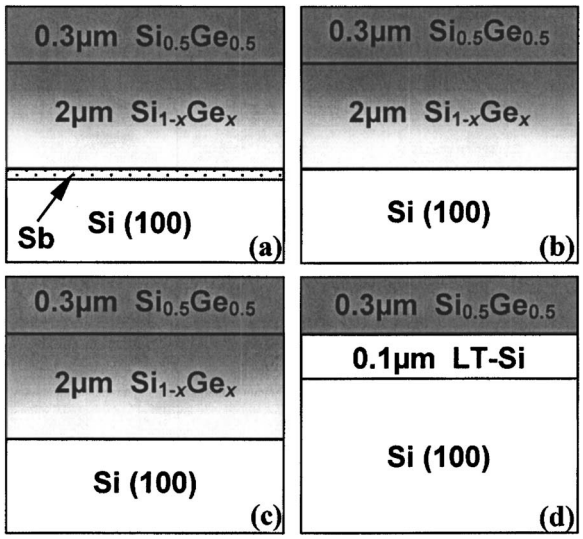

FIG. 2. Schematic diagrams of (a) JL154, 1 ML Sb was deposited before the growth of the structure, (b) JL165, the growth temperature is 700 °C, (c) JL217, the growth temperature is 510 °C, and (d) JL181, the low-temperature Si layer was grown at 200 °C, followed by SiGe deposition at 510 °C. The Ge concentration x in the SiGe buffer layers ranges from 0 at the beginning to 0.5 in the end.

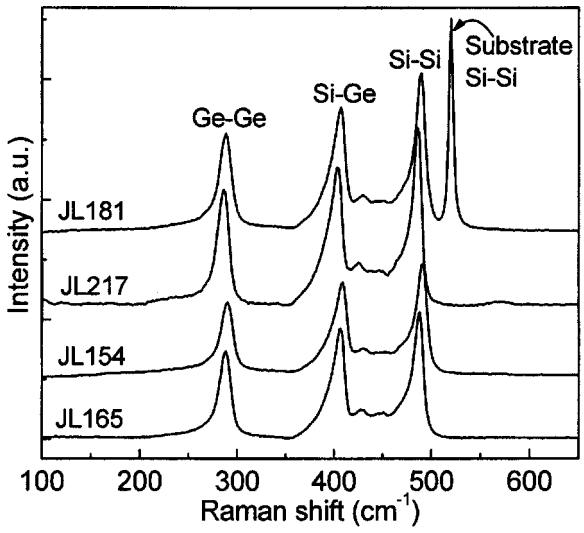

FIG. 3. Raman spectra of the four samples. JL154 is an Sb-mediated graded $Si_{0.5}Ge_{0.5}$ buffer grown at 510 °C. JL165 is a graded $Si_{0.5}Ge_{0.5}$ buffer grown at 700 °C. JL217 is a graded $Si_{0.5}Ge_{0.5}$ buffer grown at 510 °C. JL181 is a low-temperature-assisted $Si_{0.5}Ge_{0.5}$ buffer. Ge mole fraction on the top layer of each sample is determined by ω_{Si-Si} to be 0.44, 0.47, 0.5, and 0.45 for JL154, JL165, JL217, and JL181, respectively.

In order to grow high-quality Ge on Si, several methods were previously attempted. One is to grow compositionally graded SiGe layers at high temperatures (typically at 700–900 °C) with a typical grading rate of 10% Ge per 1 μm.[1] The second one is to use a low-temperature Si buffer (typically grown at 400 °C) on which a SiGe layer is grown at about 550 °C.[2] Another one is to introduce impurities, such as carbon, to adjust strain.[3] For many applications, one requires high-quality films grown on relatively thin SiGe buffer layers in order to minimize the cost. However, a relatively thin buffer fabricated by the above methods leads to a high residual strain degree, and/or a large number of threading dislocations propagating into the film on top. The structural quality of the film is degraded and the devices fabricated have poor performance.

The aim of the present paper is to systematically understand the Sb surfactant-mediated graded buffer layer growth technique, which was originally reported in Ref. 4 and leads to the growth of high-quality Ge films on Si using SiGe buffers with steep grading rates.[5] We will give quantitative explanation for the threading dislocation density reduction as a result of combining the surfactant mediation and composition grading.

II. EXPERIMENTAL RESULTS

A solid-source molecular-beam epitaxy (MBE) was used for sample growth. In order to show the effect of Sb surfactant mediation and composition grading on the quality of the SiGe films, we compared three samples having different growth conditions. Figure 2 shows the schematics of the structures. All samples have the same top-layer Ge mole fraction of 0.5. Samples JL154, JL165, and JL217 consist of a 2 μm graded SiGe with a grading rate of 25% Ge per 1 μm, followed by a 0.3 μm $Si_{0.5}Ge_{0.5}$ buffer. Sample JL154 was grown at 510 °C. One monolayer (ML) Sb was also deposited and no Sb predeposition was used for samples JL165, JL217, and JL181. Samples JL165 and JL217 were grown at 700 and 510 °C, respectively. Sample JL181 was simply a low-temperature SiGe-assisted 300-nm-thick $Si_{0.5}Ge_{0.5}$ film. The growth-temperature cycle used was the same as that in the literature.[6] The descriptions of the structures are shown in Table I.

Figure 3 shows the typical Raman spectra of the four samples. Three strong first-order peaks, i.e., Ge–Ge, Si–Ge, and Si–Si optical modes, are found for all samples. The Si–Si mode frequencies are 489.92, 488.23, 485.94, and 489.61 cm^{-1} for JL154, JL165, JL217, and JL181, respec-

TABLE I. Sample characterization data.

Sample	Raman Ge x	X-ray Ge x	X-ray Relaxation (%)	SR[a] (Å)	TD[b] (cm^{-2})	Description
JL154	0.44	0.48	96	20	1.5×10^4	Sb, graded, 510 °C
JL165	0.47	0.5	100	161	5×10^8	Graded, 700 °C
JL217	0.5	0.52	92	38	$>5\times10^8$	Graded, 510 °C
JL181	0.45	0.48	100	27	$>5\times10^8$	Low-T assisted

[a]SR: surface roughness.
[b]TD: threading dislocation density.

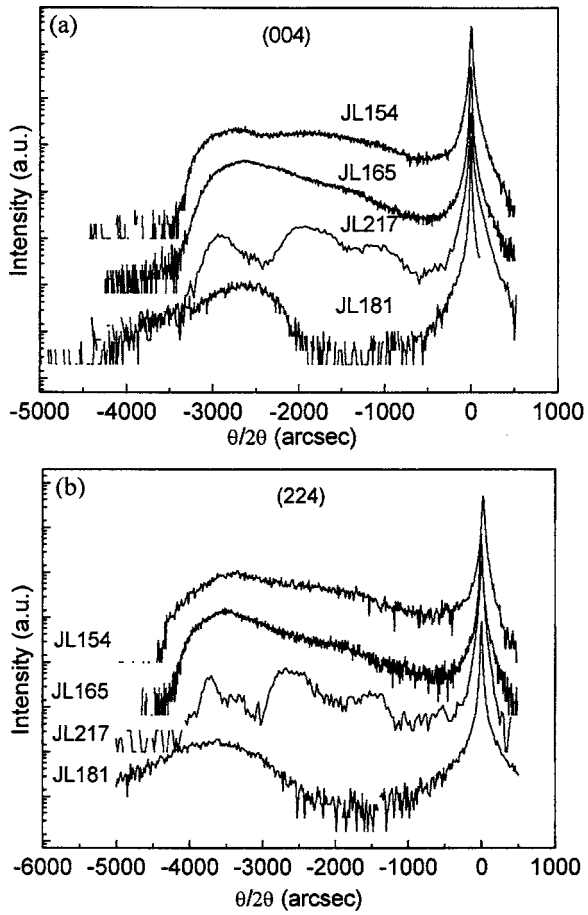

FIG. 4. X-ray (a) symmetric (004) and (b) asymmetric (224) rocking curves of the four samples, respectively. Ge mole fraction and relaxation can be obtained by the angular distances of the film peak relative to the Si substrate peak.

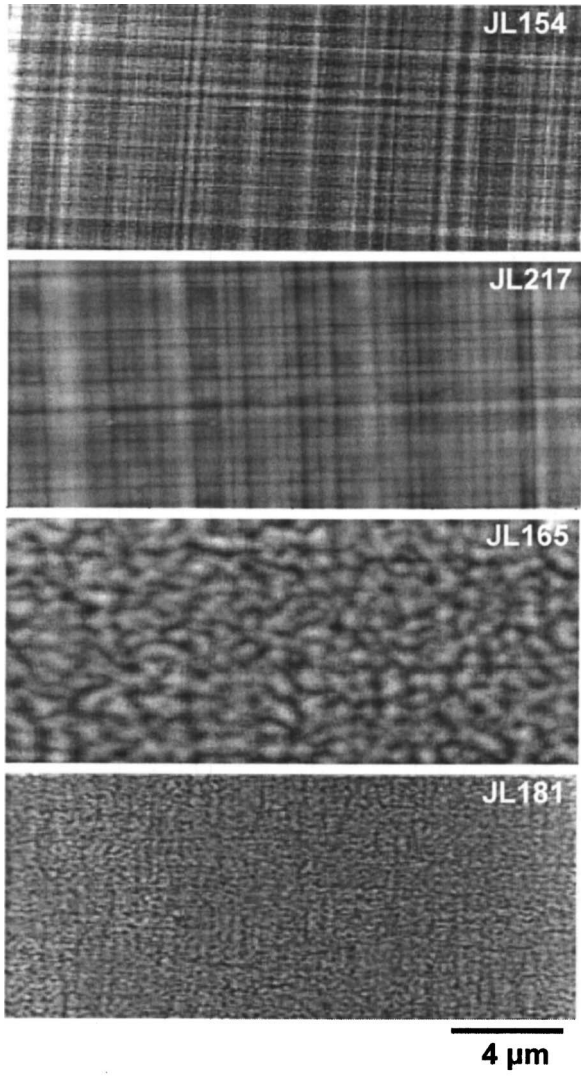

FIG. 5. AFM images of the four samples. The rms roughnesses are obtained to be 20, 161, 38, and 27 Å for samples JL154, JL165, JL217, and JL181, respectively.

tively. Considering the limited penetration depth of the Ar^+ laser used in the Raman measurements, we conclude that vibrational modes are from the top layer with constant Ge mole fraction only. Assuming that the films are fully relaxed, Ge mole fraction x of the samples can be estimated by the following equation: $\omega_{\mathrm{Si-Si}}(x)=520-68x$,[7] Ge mole fraction in the top layer of each sample was determined to be 0.44, 0.47, 0.5, and 0.45 for samples JL154, JL165, JL217, and JL181, respectively. These data are summarized in Table I.

In order to estimate both Ge mole fraction and the degree of relaxation of the films, double-axis x-ray-diffraction measurements were performed. Figures 4(a) and 4(b) show the symmetric (004) and asymmetric (224) rocking curves of the four samples, respectively. The angular distances of the film peak relative to the substrate peak in these scans are used to determine the Ge mole fraction and relaxation. The results are shown in Table I. In addition, the intensity of the layer peaks is fairly uniform up to 0.48 and 0.5 for samples JL154 and JL165, respectively, which indicates a well-controlled linear grading. For sample JL217, even though the grading process is similar to that of samples JL154 and JL165, the intensity of the layer peak does not show a uniform increase. This could be related to the film relaxation process and is explained shortly.

Surface morphology was measured with atomic force microscopy (AFM). The images are shown in Fig. 5. As one can see, long and straight cross-hatch misfit dislocation lines are observed for samples JL154 and JL217, while those of samples JL165 and JL181 are short and somehow kink, indicating very high threading dislocation densities in samples JL165 and JL181. The surface root-mean-square (rms) roughness is estimated from these AFM images to be 20, 161, 38, and 27 Å for samples JL154, JL165, JL217, and JL181, respectively.

Figure 6 shows bright-field cross-sectional transmission electron microscopy (TEM) images of the samples, respectively. For sample JL154, the dislocations occur near the bottom of the buffer and the top $Si_{0.5}Ge_{0.5}$ layer is dislocation-free. For samples JL165, JL217, and JL181, however, there are high-density threading dislocations penetrating the top $Si_{0.5}Ge_{0.5}$ layer.

In order to know the quantitative numbers of the dislocations, we used the Schimmel defect etch method followed by etch-pit counting with Nomarski microscopy.[8] The solution consisted of one part 75 g CrO_3 in 1000 ml H_2O to two parts 48% HF. Figure 7 shows Nomarski images of as-etched

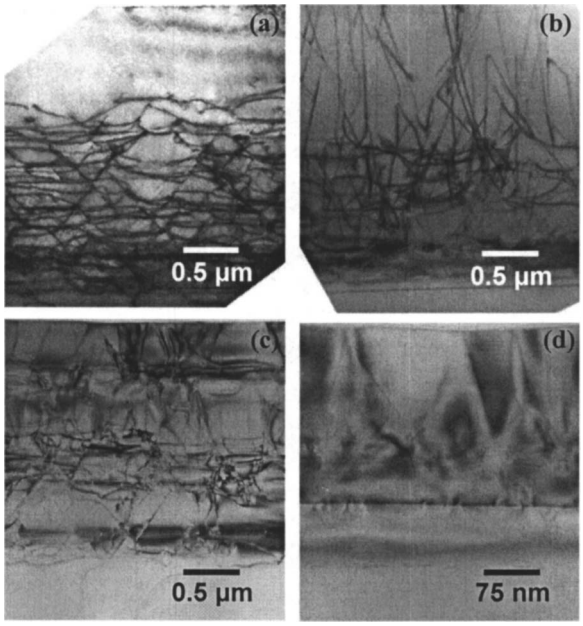

FIG. 6. Bright-field TEM images of (a) JL154, (b) JL165, (c) JL217, and (d) JL181, respectively.

samples JL154, JL165, JL217, and JL181. The etching was carried out at room temperature by dipping the composition-graded samples in the solution for 15 s and the low-temperature-assisted sample in the solution for 5 s, respectively. In the graded samples, α-step measurements indicate that almost 0.55-μm-thick material has been etched away for each sample, and thus the images were from the upper graded layers of the samples. The etching results for the samples are obviously different, and dislocation densities are summarized in Table I.

In order to gain further insight into Sb surfactant-mediated graded SiGe layers, we investigated the grading rate dependence on the threading dislocation density. A series of samples were grown by grading Ge from 0% to 50% Ge with different grading layer thickness and the same 0.2-μm-thick $Si_{0.5}Ge_{0.5}$ layer on top. An Sb layer of one ML thick was predeposited. Figure 8 shows an AFM image of an Sb-mediated $Si_{0.5}Ge_{0.5}$ sample with only 1 μm of graded layer. Even though there are long misfit dislocation lines, threading dislocations glide to the top surface and appear as dark holes. By counting the hole density, we obtain the threading dislocation density to be 2×10^8 cm^{-2}, which is the same as obtained from the etched ones.

Figure 9 shows the threading dislocation density as a function of grading rate. The threading dislocation density decreases with decreasing grading rate. For comparison, the threading dislocation densities of sample JL165 and samples from the literatures are shown.[3,9–12] All those samples were grown at higher temperatures and had the final Ge mole fraction of 0.5 at the end of the grading. For the same grading rate, for example, 50% Ge per 1 μm, the threading dislocation density for Sb-mediated samples is significantly lower than those grown at higher temperatures only.

The experiments were also performed to grow Sb-mediated graded samples at other final Ge concentrations. Figures 10(a) and 10(b) show the AFM image of the top

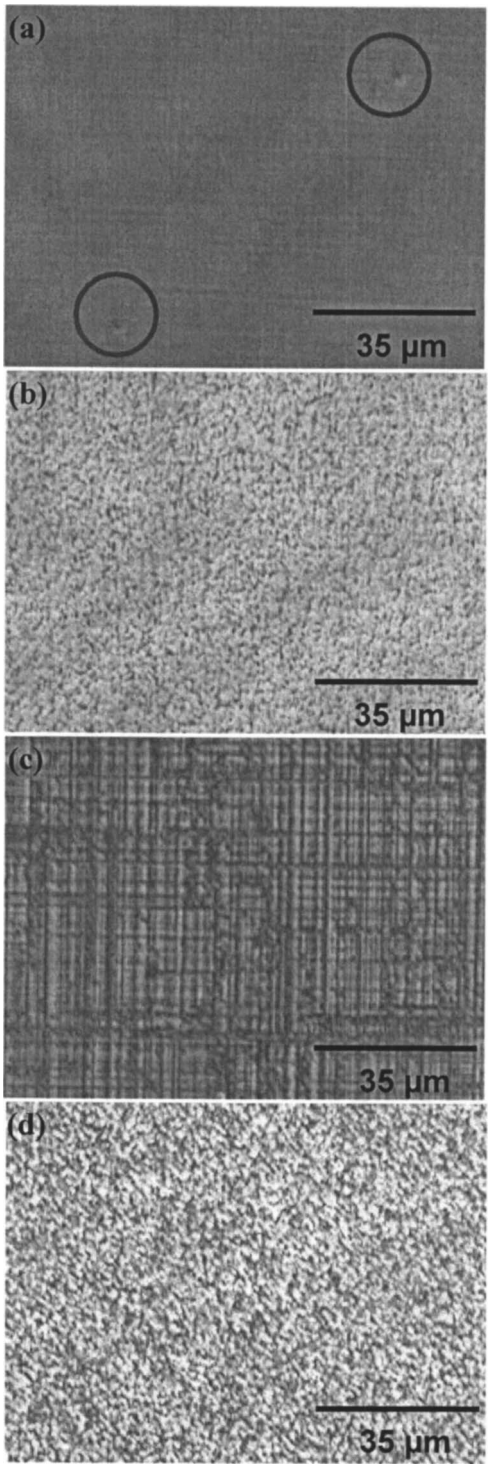

FIG. 7. The etched samples by Schimmel etchant for (a) JL154, (b) JL165, (c) JL217, and (d) JL181. Threading dislocation densities are summarized in Table I.

surface and the bright-field cross-sectional TEM image of a sample with Ge composition graded to 100%, respectively. The starting material is a p-type Si(100) with a resistivity of 15–30 Ω cm. The growth temperature was kept at 510 °C. One ML Sb was deposited immediately after the deposition of the Si buffer. The structure consists of the following layers: 100-nm-thick Si buffer, 4-μm-thick linearly graded $Si_{1-x}Ge_x$ with x from 0 to 1, and 0.9-μm-thick Ge film. Long and straight misfit dislocation lines are evident from the

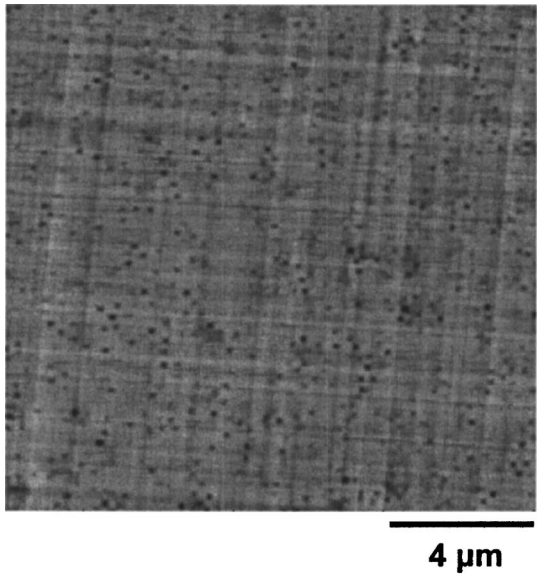

FIG. 8. AFM image of an Sb-mediated $Si_{0.5}Ge_{0.5}$ sample with only 1 μm graded layer. Threading dislocations appear as holes on the surface and the density is 2×10^8 cm^{-2}.

AFM image. The rms surface roughness was measured to be 35 Å. High-density threading dislocations are clearly seen in the graded buffer region only from the TEM image. In other words, the top 0.9 μm Ge film of high quality with a very low threading dislocation density is beyond the ability of the TEM method.

Nomarski microscopy was used to characterize defect-selectively-etched Ge samples with Sb surfactant-mediated graded buffers to obtain quantitative numbers of threading dislocations. The selective etchant was a mixture of CH_3COOH, HNO_3, HF, and I_2.[13] Threading dislocation densities were obtained by counting I-decorated pits on the surfaces. The density was characterized to be 5.4×10^5 cm^{-2} for the sample shown in Fig. 10. Figure 11 shows the comparison of the threading dislocation densities of the Ge films

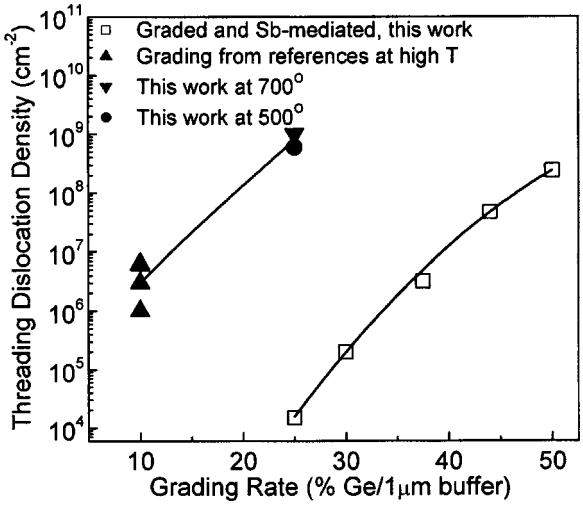

FIG. 9. Threading dislocation density as a function of grading rate of Sb-mediated graded SiGe films. The data from references are those of SiGe films grown at temperatures higher than 700 °C and without surfactant mediation. See text for references.

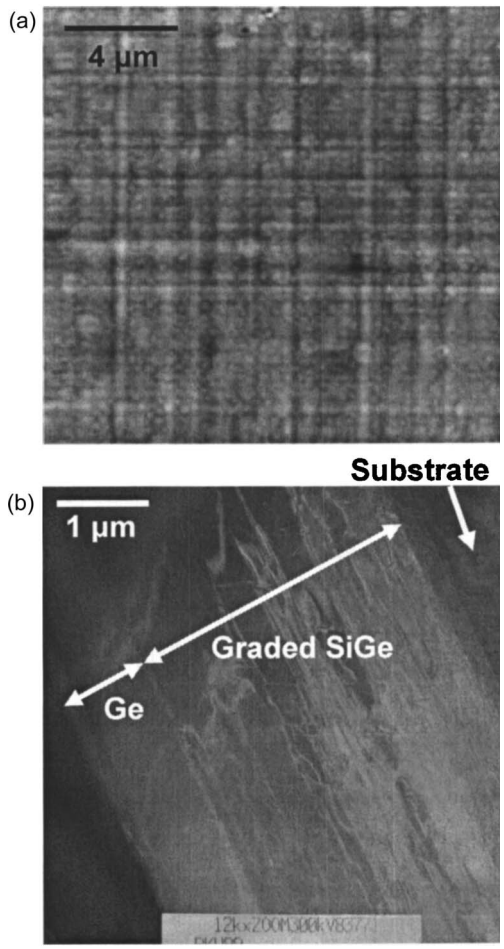

FIG. 10. (a) AFM image and (b) bright-field cross-sectional TEM image of the Ge film with Sb surfactant-mediated graded SiGe buffer. The graded layer is 4 μm thick.

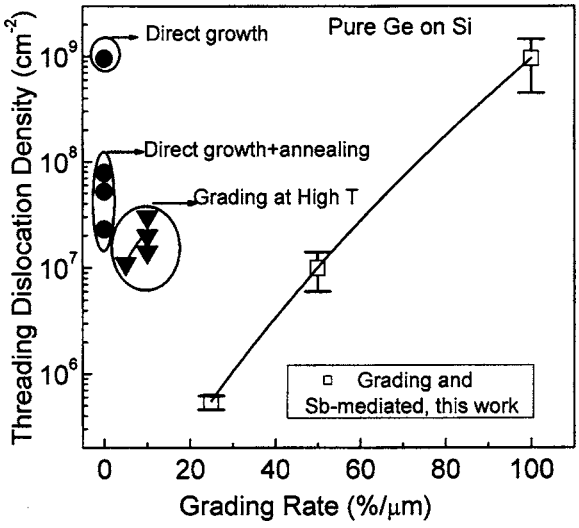

FIG. 11. Threading dislocation densities in Ge films as functions of grading rates of graded SiGe buffers underneath. The square symbols are from Sb-mediated samples. The threading dislocation density of the sample with a 4 μm buffer is estimated to be 5.4×10^5 cm^{-2} from I-coated pits. The inverted triangles represent threading dislocation densities of samples grown at temperatures higher than 700 °C from literature. The circles are threading dislocation densities of the samples with Ge directly grown on Si (the grading rate is set to be 0). See text for references.

with Sb surfactant-mediated graded buffers and other methods from the literature.[11–14] The threading dislocation densities of the samples with Sb surfactant-mediated graded buffers are less than those by other methods when the grading rate is about 50% or less. As the grading rate increases, the threading dislocation density increases for both Sb-mediated samples and those samples grown at higher temperatures.

III. DISCUSSION

It is interesting to discuss why the combination of Sb surfactant and composition grading improves the film quality markedly. For graded SiGe films grown at high temperatures ($\geqslant$700 °C), certain amounts of threading dislocations (10^6 cm^{-2} dislocation density for a graded layer with 10% Ge per 1 μm grading rate) are needed to compensate misfit strain and relax the films.[1] For relaxed SiGe films grown on low-temperature Si, the film relaxation relies on the termination of threading dislocations by point defects produced in the low-temperature Si layer.[15,16] Thus to obtain a low-dislocation-density film, a certain amount of point defects is needed in the low-temperature Si layer, which is obtained by optimizing the Si layer thickness and its growth temperature. For graded SiGe films grown only at intermediate temperatures (~500 °C), misfit dislocations cannot move effectively during film growth and once the film builds enough strain energy, it cracks abruptly by generating high-density threading dislocations. As the film continues to grow, film thickness and Ge mole fraction increase and strain builds up again. The relief of the strain will take place by generating threading dislocations again at the upper layer [clearly shown in the x-ray rocking curves of Fig. 4 and in the TEM image of Fig. 6(c)]. Graded SiGe films grown using Sb surfactant mediation at intermediate temperatures (~500 °C) have the highest quality among those by other methods.

In order to obtain a clearer picture of Sb mediation on the improvement of quality in graded SiGe films, we should address the kinetic process of strain relaxation. The strain-relaxation process of SiGe on Si has been widely discussed and may be found in the literature.[17–20] The mismatch f is always the sum of the elastic strain ε and plastic strain δ:

$$f = \varepsilon + \delta. \tag{1}$$

For a graded structure, f has a linear dependence in the growth direction, therefore we can define the grading rate C_f as

$$C_f = C_\varepsilon + C_\delta. \tag{2}$$

The elastic strain energy per unit area for a graded structure with biaxial strain is therefore[1]

$$E_\varepsilon = YC_\varepsilon^2 \int_0^h y^2 dy, \tag{3}$$

where Y is Young's modulus, h is the film thickness (graded layer), and dy is the unit thickness in the growth direction. The plastic strain energy per unit area is[1]

$$E_\delta = 2C_\delta hD\left(1 - \frac{\nu}{4}\right)\ln\left(\frac{h}{b}\right), \tag{4}$$

where $D = Gb/[2\pi(1-\nu)]$, G is the shear modulus, ν is Poisson's ratio, and b is the magnitude of the Burgers vector. The total energy of the system is

$$E_{\text{total}} = E_\varepsilon + E_\delta. \tag{5}$$

This energy can then be minimized with respect to the elastic strain slope C_ε. This minimization defines the critical thickness at which threading dislocations are introduced:

$$h_C^2 = \frac{3D[1-(\nu/4)]\ln(h_C/b)}{YC_\varepsilon}. \tag{6}$$

For film thickness larger than h_C, the equilibrium plastic strain gradient in the graded region is therefore

$$C_\delta = C_f - \frac{3D[1-(\nu/4)]\ln(h/b)}{Yh^2}. \tag{7}$$

At great thickness, the second term in the above equation is very small compared with the first term at the right-hand side, therefore

$$C_\delta \approx C_f. \tag{8}$$

The plastic strain in a graded film of thickness h is simply

$$\delta = C_\delta h = C_f h. \tag{9}$$

The first derivative of δ, i.e., the plastic strain rate, is therefore

$$\dot{\delta} = C_f \frac{\Delta h}{\Delta t} = C_f R_{\text{gr}}, \tag{10}$$

where R_{gr} is the growth rate. If the density of threading dislocations is ρ, the plastic strain rate can be expressed by[1]

$$\dot{\delta} = \tfrac{1}{2}\rho b v, \tag{11}$$

where v is the average misfit dislocation velocity. Empirically, v is expressed by[19]

$$v = v_0\left(\frac{\tau_{\text{eff}}}{G}\right)^m \exp\left(-\frac{Q_a}{kT}\right), \tag{12}$$

where τ_{eff} is the effective stress[21] and v_0 and m are material constants. Q_a is the activation energy for dislocation glide. By combining Eqs. (10)–(12), one can easily obtain

$$\rho = \frac{2R_{\text{gr}}}{bv}C_f = \frac{2R_{\text{gr}}}{bv_0}\left(\frac{\tau_{\text{eff}}}{G}\right)^{-m} C_f \exp\left(\frac{Q_a}{kT}\right). \tag{13}$$

The effective stress τ_{eff} is also a function of grading rate and can be fitted by[22]

$$\tau_{\text{eff}} = \exp(a_0 + a_1 C_f + a_2 C_f^2), \tag{14}$$

where a_0, a_1, and a_2 are constants. Substituting this equation into Eq. (13), we obtained

$$\rho(C_f) = C_f \exp(P_0 + P_1 C_f + P_2 C_f^2), \tag{15}$$

where P_0, P_1, and P_2 are fitting parameters that are related to the growth temperature, activation energy, and other material constants. The fitting results are shown as solid lines in Figs.

TABLE II. Fitting parameters for threading dislocation density as a function of grading rate in Figs. 9 and 11.

Final	Ge of graded layers	P_0	P_1	P_2
0.5	With Sb	−9.456 18	0.775 32	−0.005 57
0.5	Without Sb	9.525 18	0.307 56	0.000 11
1	With Sb	−7.625 97	0.098 79	−0.000 14
1	Without Sb	14.603 62	0.000 11	0

9 and 11 with the fitting parameters summarized in Table II. The dislocation density indeed increases as the grading rate C_f increases, and the fitting results are in excellent agreement with experimental data trends. The threading dislocation density difference between the graded buffers at high temperatures and the Sb surfactant-mediated graded layers arises from the different set of fitting parameters, which are related to the growth temperature activation energy, etc. If we neglect the effect from P_2 as both P_0 and P_1C_f are much larger than $P_2C_f^2$ from our fitting and assume that other material constants are the same for both Sb surfactant-mediated and nonsurfactant-mediated graded layers, we expect a smaller activation energy for dislocation glide in Sb surfactant-mediated graded layers as these samples were grown at lower temperatures. This means that dislocations are easier to glide in the graded layers with the presence of a surfactant. It should be noted that the concept of a surfactant is a modification of the surface of an epitaxial layer during growth.[23–25] The effect of the surface energy modification as a result of Sb surfactant mediation on the bulk property of dislocation glide (easier glide observed in the Sb surfactant-mediated graded layers) is not clear and needs further studies.

IV. APPLICATION

The above Sb surfactant-mediated SiGe graded buffer layer technique can be used to grow high-quality SiGe-based films and quantum structures for many applications. Here we only show our results of Ge photodetectors on Si substrates for 1.3–1.55 μm optical communication applications.[26]

The starting structure is similar to that shown in Fig. 10, except that the top 0.6-μm- thick buffer was doped with Sb of 0.7×10^{17} cm^{-3} to form the n layer and the top 0.1-μm-thick Ge layer was doped with B of 5×10^{18} cm^{-3} to form the p layer. The samples were fabricated into Ge p-i-n mesa diodes with different mesa sizes. Ti/Au was used as contact material. Figure 12 shows typical I-V measurement results of three diodes with different mesa sizes at room temperature. Rectifying behaviors are observed. A detailed investigation of the scaling characteristics of reverse currents at −1 V for many devices displayed a proportionality of currents with the mesa sizes, indicating that leakage is not caused by edge effects but related to material quality only. The dark current density at a reverse bias of 1 V was determined to be about 0.15 mA/cm^2 for many devices. This result was orders of magnitude lower than the previously reported dark currents of 200 mA/cm^2 (Ref. 27) and 50 mA/cm^2 (Ref. 28) and only four times larger than the ideal dark diffusion current based on our doping profile.

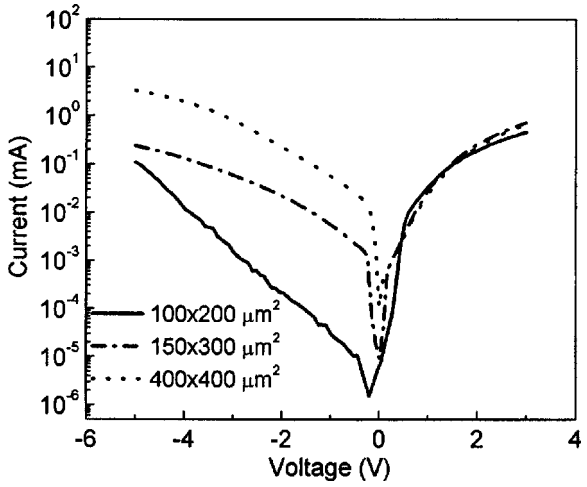

FIG. 12. I-V characteristics of p-i-n Ge diodes with different mesa sizes. The reverse current scales with the area of the mesa, suggesting that the dark current mainly originates from the Ge material only rather than an edge effect. The dark current densities are determined to be about 0.15 mA/cm^2 at the reverse bias of 1 V.

Besides I-V characteristics, we also measured C-V characteristics, which were not shown here. The capacitance of an ideal p-i-n diode is $(A/C)^2=(2/qN\varepsilon)(V+V_{bi})+(W^2/\varepsilon^2)$,[27] where N is the density of fixed charges at one of the boundaries of the depletion layer, W is the i- layer thickness, ε is the dielectric permittivity, V is the reverse bias, and V_{bi} is the built-in potential related to the doping density. For a diode with 100×200 μm^2 mesa size, the measured capacitance indeed decreases as the reverse bias increases, however, the data trend of C^{-2} does not show linear dependence with voltage, suggesting that the doping is not abrupt as a result of the segregation of Sb during the n-type layer doping. The capacitance is determined to be about 0.6 pF at −5 V. Such a small capacitance for this big diode suggests that smaller mesa diodes would be promising for high-speed fiber-optic communication applications. Nevertheless, due to the low-density n-type doping underneath the intrinsic layer, the contact/series resistance is so large, which can be seen from forward I-V characteristics as well, that our measured 3 dB bandwidth for these detectors is less than 1 GHz. The improved frequency response could be achieved by using phosphor doping instead of Sb doping in the n-type layer region and by optimizing the diode structure with contact pads closer to mesas.

Figure 13 shows the photoresponse versus the wavelength of incident light for three different reverse biases measured at room temperature. No antireflection film coating was deposited. The data were not corrected for the spectral variation of the incident optical power of the tungsten source used in the experiment. The photocurrent threshold at about 1.6 μm agrees with the well-known absorption data for Ge.[29] The spectrum at 0 V suggests that the devices can be operated in the photovoltaic mode. The higher photocurrents at higher reverse biases arise from two possibilities. First, the intrinsic region (space-charge region) is slightly enlarged at higher reverse biases, therefore more photogenerated carriers are generated. Second, the photogenerated carriers are swept by the electrode more efficiently due to a higher electric field

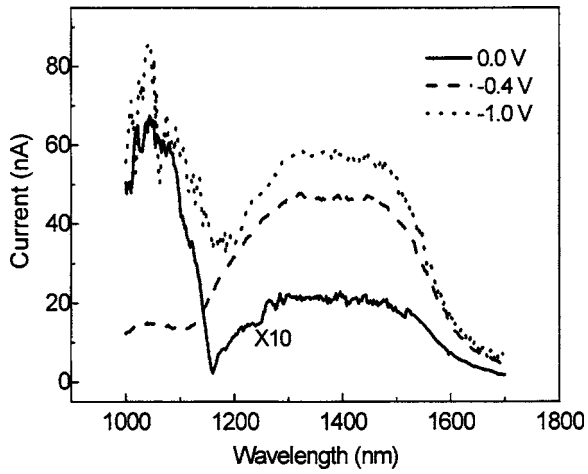

FIG. 13. Photoresponse spectra for a Ge photodiode with a mesa size of 150×300 μm^2 measured at different reverse biases.

in the intrinsic region at a higher bias. This is because the drift velocity of the photogenerated carriers in the intrinsic layer is higher at higher electric field. Thus the transit time is lower and the carriers have a lesser possibility to recombine before they reach the electrodes, suggesting that more carriers per unit time can be collected at the electrodes. The response at about 1.1 μm is from the Si substrate and SiGe buffer layer. It is not difficult to understand this if we realize that the *p*-type Si substrate is used. Such design is typical in integrated photonics systems as there is a *p-n* junction formed by the *n*-type doping SiGe graded layer and the *p*-type Si substrate underneath for electrical isolation. During the measurements, the photogenerated carriers in the Si layer (space-charge region is in the Si substrate due to a lower doping concentration in the substrate) are simultaneously collected by the metal contact on the surface.

The quantum efficiency is one of the important figures of merit of a photodetector. The quantum efficiency can be estimated as $\eta=I_P h\upsilon/qP$, where I_P is the photocurrent, $h\nu$ is the photoenergy as defined by the wavelength, and P is the incident optical power. By using a commercialized 1.55-μm-wavelength laser and a calibrated Ge photodetector, the quantum efficiencies for many devices are in the region of 50%–72% at the reverse bias of 1 V.

V. SUMMARY

The quality of SiGe and Ge thin films grown on a Si substrate by MBE was further improved by using Sb surfactant-mediated SiGe graded buffer layers compared with the conventional SiGe graded buffer method. Both transmission electron microscopy and Schimmel defect etch measurements show that the Sb surfactant-mediated SiGe graded buffer layers have lower dislocation densities than those without an Sb surfactant. A systematic study of Sb surfactant-mediated buffer layers was performed. The results suggest that the Sb surfactant-mediated graded layers have a smaller activation energy for threading dislocations to glide, leading to lower threading dislocation densities in the upper layers, compared with those graded buffers without surfactant mediation. Moreover, we demonstrated high-performance Ge *p-i-n* photodiodes grown using the combination of Sb surfactant mediation and graded buffer technique. These Ge *p-i-n* diodes show a very low dark current density of about 0.15 mA/cm^2 at the reverse bias of 1 V and a quantum efficiency of around 50%–72%. The results suggest the potential applications of such Ge detectors for monolithically integrated photoreceivers on Si substrates.

ACKNOWLEDGMENTS

The authors are grateful to M. Goorsky, T. Radetic, R. Gronsky, D. P. Yu, S. G. Thomas, and S. Tong, for technical assistance in XRD, TEM, and photoresponse characterizations. This work was partially supported by DARPA/DMEA through CNID.

[1] E. A. Fitzgerald, Y.-H. Xie, D. Monroe, P. J. Silverman, J. M. Kuo, A. R. Kortan, F. A. Thiel, and B. E. Weir, J. Vac. Sci. Technol. B **10**, 1807 (1992).
[2] J. H. Li, C. S. Peng, Y. Wu, D. Y. Dai, J. M. Zhou, and Z. H. Mai, Appl. Phys. Lett. **71**, 3132 (1997).
[3] H. J. Osten and E. Bugiel, Appl. Phys. Lett. **70**, 2813 (1997).
[4] J. L. Liu *et al.*, Appl. Phys. Lett. **75**, 1586 (1999).
[5] J. L. Liu, S. Tong, Y. H. Luo, J. Wan, and K. L. Wang, Appl. Phys. Lett. **79**, 3431 (2001).
[6] M. Bauer, K. Lyutovich, M. Oehme, E. Kasper, H.-J. Herzog, and F. Ernst, Thin Solid Films **369**, 152 (2000).
[7] J. C. Tsang, P. M. Mooney, F. Dacol, and J. O. Chu, J. Appl. Phys. **75**, 8098 (1994).
[8] D. Schimmel, J. Electrochem. Soc. **126**, 479 (1979).
[9] E. A. Fitzgerald, Y.-H. Xie, M. L. Green, D. Brasen, A. R. Kortan, J. Michel, Y.-J. Mii, and B. E. Weir, Appl. Phys. Lett. **59**, 811 (1991).
[10] E. A. Fitzgerald, M. T. Currie, S. B. Samavedam, T. A. Langdo, G. Taraschi, V. Yang, C. W. Leitz, and M. T. Bulsara, Phys. Status Solidi A **171**, 227 (1999).
[11] S. B. Samavedam and E. A. Fitzgerald, J. Appl. Phys. **81**, 3108 (1997).
[12] M. T. Currie, S. B. Samavedam, T. A. Langdo, C. W. Leitz, and E. A. Fitzgerald, Appl. Phys. Lett. **72**, 1718 (1998).
[13] H. C. Luan, D. R. Lim, K. K. Lee, K. M. Chen, J. G. Sandland, K. Wada, and L. C. Kimerling, Appl. Phys. Lett. **75**, 2909 (1999).
[14] C. Rosenblad, H. V. Kanel, M. Kummer, A. Dommann, and E. Muller, Appl. Phys. Lett. **76**, 427 (2000).
[15] J. H. Li, C. S. Peng, Y. Wu, D. Y. Dai, J. M. Zhou, and Z. H. Mai, Appl. Phys. Lett. **71**, 3132 (1997).
[16] Y. H. Luo, J. Wan, R. L. Forrest, J. L. Liu, G. Jin, M. S. Goorsky, and K. L. Wang, Appl. Phys. Lett. **78**, 454 (2001).
[17] E. A. Fitzgerald, Mater. Sci. Rep. **7**, 87 (1991).
[18] R. Hull and J. C. Beam, Crit. Rev. Solid State Mater. Sci. **17**, 507 (1992).
[19] D. C. Houghton, J. Appl. Phys. **70**, 2136 (1991).
[20] A. M. Anfrew, J. S. Speck, A. E. Romanov, M. Bobeth, and W. Pompe, J. Appl. Phys. **91**, 1933 (2002).
[21] J. W. Matthews, S. Mader, and T. B. Light, J. Appl. Phys. **41**, 3800 (1970).
[22] E. A. Fitzgerald, A. Y. Kim, M. T. Currie, T. A. Langdo, G. Taraschi, and M. T. Bulsara, Mater. Sci. Eng., B **67**, 53 (1999).
[23] E. Tournie and K. H. Ploog, Thin Solid Films **231**, 43 (1993).
[24] M. Horn-von Hoegen, B. H. Muller, and A. Al-Falou, Phys. Rev. B **50**, 11640 (1994).
[25] M. Horn-von Hoegen, M. Copel, J. C. Tsang, M. C. Reuter, and R. M. Tromp, Phys. Rev. B **50**, 10811 (1994).
[26] J. L. Liu *et al.*, Thin Solid Films **380**, 54 (2000).
[27] S. Luryi, A. Katalsky, and J. C. Bean, IEEE Trans. Electron Devices **31**, 1135 (1984).
[28] P. Sutter, U. Kafader, and H. von Kanel, Sol. Energy Mater. Sol. Cells **31**, 541 (1994).
[29] S. M. Sze, *Physics of Semiconductor Devices*, 2nd ed. (Wiley, New York, 1981).